Scientia Iranica, Vol. 10, No. 1, pp 103–109

SCIENTIA
IRANICA

Research Note

Thermoelastic Contact Analysis of a Welded Monolayer Pressure Vessel Using Interface Elements

G. Karami* and F. Niknam Moghadam[1]

In this paper, the implementation of an interface element to model the contact between the core and the layer in thermoelastic contact analysis of monolayer pressure vessels is presented. How to couple the elements of the core and the layer and implementation of the boundary conditions are also described. The source of heat could be due to temperature difference in the layers in practice or the heat due to welding in the concentrated welding zone of the layer during the assemblage of the layer and the core of the pressure vessel. Thermoelastic contact between the core and layer has come under investigation. It is concluded that the methodology with the special employment of interface elements in joints and contact regions is efficient for analysis of joints and contact problems in the analysis of layered media.

INTRODUCTION

With the increasing demands of industrial processes to obtain higher operating pressure, multilayer prestressed vessel construction has come under (Figure 1) investigation in recent year. Layered vessels are being widely used because of their flexibility in manufacturing and their safety behavior in operation. The higher safety aspects of a layered structure have also been proved in practice.

In a monolayer pressure vessel, a longitudinal welded layer tightly wraps the core cylinder. The wrapping process, as well as the shrinkage of a longitudinal weld at the layer, induces a compressive prestress at the vessel's core, which can reduce the tensile stress due to the application of internal pressure. The circumferential shrinkage of a wrapped layer, due to cooling of the weld, is related to the corresponding radial interference and the resulting residual compressive stresses being developed.

In 1985, Srinivasan and France [1] developed a computer simulation of a duplex tube, including the effect of thermal expansion using empirically obtained data for the influence of contact pressure on the interface thermal resistance. Rasty and Sabbaghian [2] have reported an analytical solution for the determination of the magnitude of prestress throughout the wall thickness of a monolayered wrapped vessel in 1988. In 1990, Wang et al. [3] carried out a theoretical and experimental analysis for determination of the highest risk of longitudinal welds in a wrapped multilayer vessel. They assumed all internal length-wise seams unwelded except for the innermost and the outermost layers. The friction between layers is also investigated. In 1990, Jahanian and Sabbaghian [4] developed a

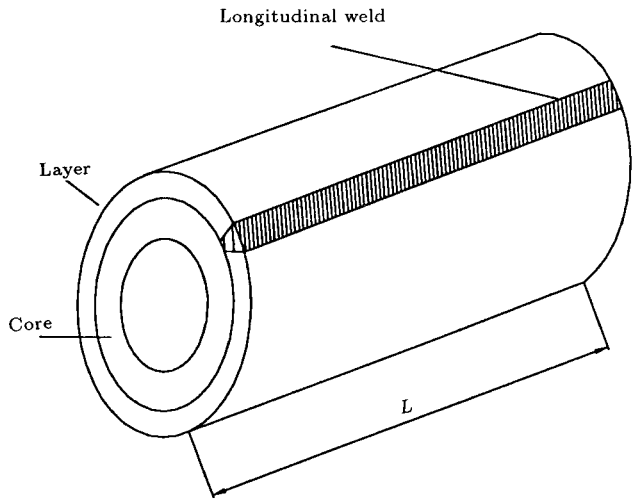

Figure 1. A monolayer pressure vessel.

*. *Corresponding Author, Department of Mechanical Engineering, School of Engineering, Shiraz University, Shiraz, I.R. Iran.*

1. *Department of Mechanical Engineering, School of Engineering, Shiraz University, Shiraz, I.R. Iran.*

theoretical study of the stresses in a long hollow circular cylinder subjected to rapid cooling of the exterior surface. In 1994, Rasty and Tamhane [5] employed a finite element package ABAQUS to calculate the prestress in a monolayer pressure vessel. A solution has been presented for the stresses and displacements which take place in hollow circular cylinders subjected to asymmetric temperature by Zibdeh and Al Farran [6] in 1995.

In this paper, a two-dimensional finite element algorithm is used as a numerical tool for thermoelastic contact analysis in a monolayer pressure vessel. To model the interface between the layer and core, a special element, called the interface element, is developed.

THERMOELASTIC FORMULATION

The boundary value problem under consideration combines the theories of elasticity and of heat conduction under transient conditions [7]. For a body with the density of ρ, specific heat c_E, thermal conductivity k and the Lame constants λ and μ, the linear thermoelastic theory states that:

$$KT_{,ii} = \rho c_E \dot{T} + (3\lambda + 2\mu)\alpha T_0 \dot{\varepsilon}_{kk}. \tag{1}$$

The equation of motion in an elastic body is written;

$$\sigma_{ij,j} + \rho F_i = \rho \ddot{u}_i, \tag{2}$$

where, σ_{ij} is the stress tensor and F_i is the body force per unit mass. By neglecting inertia terms in Equation 2, the coupled thermoelastic Equation 1 may be rewritten as:

$$KT_{,ii} = \rho c_E \dot{T}\left[1 + \delta\left(\frac{\lambda + 2\mu}{3\lambda + 2\mu}\right)\left(\frac{\dot{\varepsilon}_{kk}}{\alpha \dot{T}}\right)\right], \tag{3}$$

where c_E is known as the specific heat at constant deformation of the elastic solid and the nondimensional parameter δ is defined as $\delta = \frac{(3\lambda+2\mu)^2\alpha^2 T_0}{\rho^2 c_\nu V_e^2}$. T_0 is the initial temperature, c_ν is the heat capacity per unit temperature and ν_e is the velocity of propagation of dilational waves in an elastic medium being calculated by, $\nu_e = \sqrt{\frac{(\lambda+2\mu)}{\rho}}$. The term proportional to δ in the above equation is the coupling term and it is negligible compared to unity if:

$$\frac{\dot{\varepsilon}_{kk}}{3\alpha \dot{T}} << \left(\frac{\lambda + 2\mu/3}{\lambda + 2\mu}\right)\left(\frac{1}{\delta}\right). \tag{4}$$

For temperature distribution with no sharp variations or discontinuities in their time history, it is intuitively expected that the time rate of change of the dilatation is of the same order of magnitude as that of the temperature; thus, disregard of coupling as described previously, appears to be reasonable. With the omission of coupling, the general thermal stress problem separates into two distinct problems to be solved consecutively and the second is the determination of the resulting stress distribution.

INTERFACE ELEMENT FORMULATIONS

Interface elements are those kinds of elements that are employed at the interface of two domains having relative movement with respect to each other [8,9]. A general and an 'accurate formulation of the stiffness matrix for an interface element were introduced by Yuan and Chua [10].

Following the conventional displacement formulation in finite element analysis, the stiffness matrix $[K]$ of the interface element in the local coordinate system is usually written as:

$$[K] = \int_V [B]^T [C] [B] \, dV, \tag{5}$$

where $[B]$ is the strain-displacement matrix and $[C]$ is the constitutive matrix. For the four-noded interface element shown in Figure 2, the thickness of the element is assumed to be small in comparison with its length and, as such, the stress and strain are assumed to be uniform across the entire thickness.

The shape function of such elements can be expressed as one-directional interpolation functions along the surface of the element by:

$$N_1 = \frac{1}{2}(1 - \frac{2\zeta}{L}), \quad N_2 = \frac{1}{2}(1 + \frac{2\zeta}{L}). \tag{6}$$

As the thickness is very small, the relation between the strain vector and the nodal displacement vector may

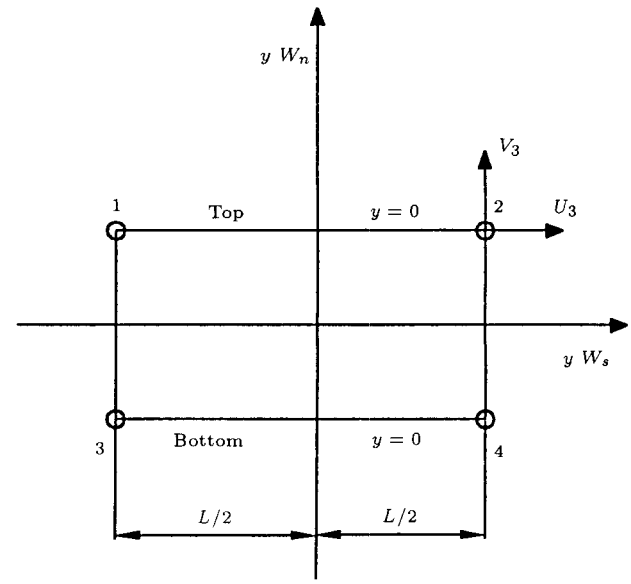

Figure 2. Schematic diagram of 2-D interface element.

be written as:

$$[B]\{u\} = \frac{1}{t}\begin{bmatrix} -N_1 & 0 & -N_2 & 0 & N_2 & 0 & N_1 & 0 \\ 0 & -N_1 & 0 & -N_2 & 0 & N_2 & 0 & N_1 \end{bmatrix} \begin{Bmatrix} u_1 \\ \nu_1 \\ u_2 \\ \nu_2 \\ u_3 \\ \nu_3 \\ u_4 \\ \nu_4 \end{Bmatrix}, \quad (7)$$

where $\{u\}$ is the nodal displacement vector with components u_i, ν_i are the nodal degrees of freedom or displacement and t is the thickness of the element. Since the interface element represents the interaction characteristics between two materials, there exist an uncoupled normal stress, σ and a shear stress τ in the interface domain. The stress and strain relation for the interface domain may be written as:

$$\begin{Bmatrix} \tau \\ \sigma \end{Bmatrix} = \begin{bmatrix} k_s & 0 \\ 0 & k_n \end{bmatrix} \begin{Bmatrix} \gamma \\ \varepsilon \end{Bmatrix}, \quad (8)$$

where k_s is the interface shear stiffness and k_n is the interface normal stiffness. The elastic constitutive matrix $[C]$ is thus, $[C] = \begin{bmatrix} k_s & 0 \\ 0 & k_n \end{bmatrix}$. Substituting for $[B]$ and $[D]$ into Equation 6 and eliminating the thickness term t, gives:

$$[K] = L/4 \times \begin{bmatrix} C_1k_s & 0 & C_2k_s & 0 \\ 0 & C_1k_n & 0 & C_2k_n \\ C_2k_s & 0 & C_3k_s & 0 \\ 0 & C_2k_n & 0 & C_3k_n \\ -C_2k_s & 0 & -C_3k_s & 0 \\ 0 & -C_2k_n & 0 & -C_3k_n \\ -C_1k_s & 0 & -C_2k_s & 0 \\ 0 & -C_1k_n & 0 & -C_2k_n \end{bmatrix} \begin{bmatrix} -C_2k_s & 0 & -C_1k_s & 0 \\ 0 & -C_2k_n & 0 & -C_1k_n \\ -C_3k_s & 0 & -C_2k_s & 0 \\ 0 & -C_3k_n & 0 & -C_2k_n \\ C_3k_s & 0 & C_2k_s & 0 \\ 0 & C_3k_n & 0 & C_2k_n \\ C_2k_s & 0 & C_1k_s & 0 \\ 0 & C_2k_n & 0 & C_1k_n \end{bmatrix}, \quad (9)$$

where C_1, C_2 and C_3 are geometrical constants.

MATERIAL PROPERTIES OF THE INTERFACE ELEMENT

The properties that may be assigned to nodal joints consist of shearing and normal stiffnesses of the joints. They correspond physically to the stiffness and strength of the fault gauge, to the roughness of the joints and the angles of slip surface relative to the principal plane of the joint. They are classed as dilatant if shearing produces joint expansion or contraction or nondilatant if shearing and normal displacements are uncoupled. It is convenient to specify the properties in natural coordinates, which may be directions parallel and perpendicular either to the slip surface or the principal plane of the joint.

Nondilatant Joints

In this class of joints, there is no volume change due to shearing strains and, therefore, the shear and normal components of deformation are uncoupled and the stress-strain relations are as those given in Equation 9, where k_n and k_s are nonlinear functions.

Ghaboussi et al. [9] carried out research into the values of normal and shear stiffness. In relating stress to deformation in the direction normal to the joint, three distinct stages are defined (Figure 3):

- In separation, $k_n = k_s = 0$ when $\varepsilon \geq 0$.
- In the crushing of surface irregularities or in the compression of material at the fault or joint, if any, $k_n = E(\varepsilon_n^c \leq \varepsilon_n \leq 0)$. For smooth surfaces this case does not exist, therefore, $\varepsilon_n^c = 0$.
- In contact, $k_n = E_f(\varepsilon_n \leq \varepsilon_n^c)$. Very high values can be assigned to E_f without any numerical problems with the special joint element.

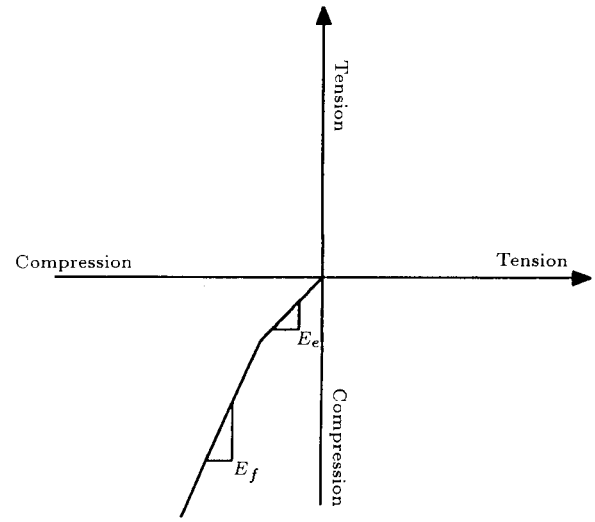

Figure 3. Normal stress-strain relation for joints.

The tangential stress-strain relationship is assumed to be elastic-perfectly plastic using a Mohr-Coulomb yield criterion, thus:

For elastic, $k_s = G$ for $\sigma_s < c + \sigma_n \tan(\phi)$,

For plastic, $k_s = 0$ for $\sigma_s = c + \sigma_n \tan(\phi)$,

in which c and ϕ are the cohesion and the angle of friction, respectively.

ASSEMBLAGE OF INTERFACE AND DOMAIN ELEMENTS STIFFNESS

The interface elements stiffnesses should be assembled to the domain elements, so that the composed system should be solved subject to the external excitations of either the thermal and/or mechanical loadings. In the cases of both heat transfer and stress analyses, these interface elements will play a role if interfaced between the layer and core of the body.

The uncoupled thermoelastic analysis procedure in this work is summarized as follows:

- To compute and measure temperature distribution, a heat transfer analysis is carried out primarily. Both domains and interface elements are discretized. Heat transfer elements are used in the domains and convection heat transfer interface elements are employed to model the interface;
- Once the temperature is known, the thermoelastic analysis would then be carried out. Again, two-dimensional elements are used to model the domain of the layer and body and special interface elements are employed to model the contacting region of the two layers of domains.

THERMOELASTIC CONTACT ANALYSIS OF THE MONOLAYER PRESSURE VESSELS

The problem under consideration in this paper involves finding the solution to the temperature, displacement, deformation and stresses in a body that is subjected to some history of loading. The displacement finite element method is based on approximating the previously stated equilibrium requirement by replacing it with a weaker requirement, so that the equilibrium must be maintained, in an average sense, over a finite number of divisions of the body. The core cylinder, with an inside radius of 0.762 m and a thickness of 12.7 mm was assumed to be stress-free before the addition of the first layer. A 6.4 mm thick layer of steel sheet was assumed to have been wrapped around the core and then welded along a longitudinal seam. The width of the weld was taken as 7.6 mm (Figure 4). Initially, the weld was assumed to be at a temperature of 1132°C (2070°F) and the rest of the layer plate to be at 21°C (70°F). The added layer plate was also assumed to be stress-free prior to the cooling of the weld.

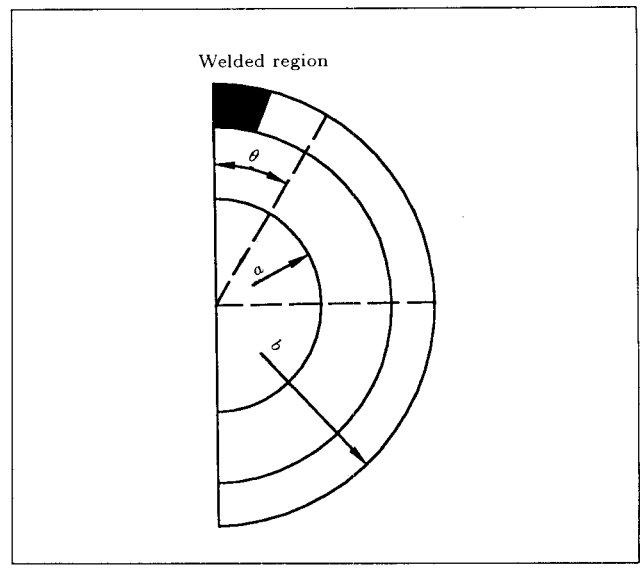

Figure 4. A monolayer pressure vessel (case study).

Table 1. Material properties for the monolayer pressure vessel.

Material Property	Value
Density (ρ)	7832 kg/m^3
Specific heat (c)	434 J/kg°K
Thermal conductivity (k)	63.9 W/m°K
Coefficient of thermal exp. (α)	12.51 mm/mm°C
Modulus of elasticity (E)	207 Gpa
Poisson's ratio (ν)	0.3

The material used in the simulation was carbon steel. The material property is shown in Table 1. In the ensuring analysis, plane strain condition is assumed. Both the core and the layer around it are free of stress prior to the cooling of the weld. At first only the welded segment of the layer is assumed to be at 1132°C (2070°F) and the rest of the layer, as well as the core, are at 21°C (70°F). Materials were assumed to be homogeneous, isotropic and linear elastic. Material properties such as conductivity, coefficient of thermal expansion, Young's modulus and specific heat are constant and do not vary with temperature. Heat transfer coefficient is constant. Calculations are representative of the middle portion of the vessel and do not reflect closure or other discontinuous effects. Elements used for modeling are isotropic linear triangular type elements.

THE MODELING PROCEDURE

Due to symmetry of the problem, only half of the cross section was modeled, utilizing 108 nodes and 134 elements. The mesh in the weld region is refined

to accommodate large gradients. 17 two-dimensional interface elements are used between the core and the layer. Figure 5 shows the finite element model, with an enlarged view of the weld region. The shaded elements represent the weld.

The total degrees of freedom were 108 for the heat transfer analysis and 216 for the thermal stress analysis. The following boundary conditions were applied to the heat transfer analysis:

- Because of symmetry, the heat flux at the two ends of the half vessel vanishes, thus:

  $Q = 0, \quad \text{for} \quad t > 0.$

- There is heat loss from the inner and outer surfaces of the cylinder to the outside by means of heat convection:

  $Q - h\Delta T = 0, \quad \text{for} \quad t > 0.$

  The value of h, the heat transfer coefficient, was calculated by the simplified formula used for natural convection [11],

  $$h = 0.27(\Delta T)^{(0.25)}, \quad \text{W/m}^2\text{°K},$$

  where ΔT is the Farenheit temperature difference between the surface of the body and the bulk of the gas surrounding it. With $\Delta T = 1093$°C (2000°F), for this model, h comes out to be 10.25 W/m^2°K;

- The layer coming in contact with the core cylinder introduces thermal resistance. At the interface of the layer and the core cylinder, the thermal resistance introduces the following condition for the heat flux, being equal to the temperature difference across the surface [12]:

  $$Q = \frac{1}{R}(\Delta T), \quad T > 0.$$

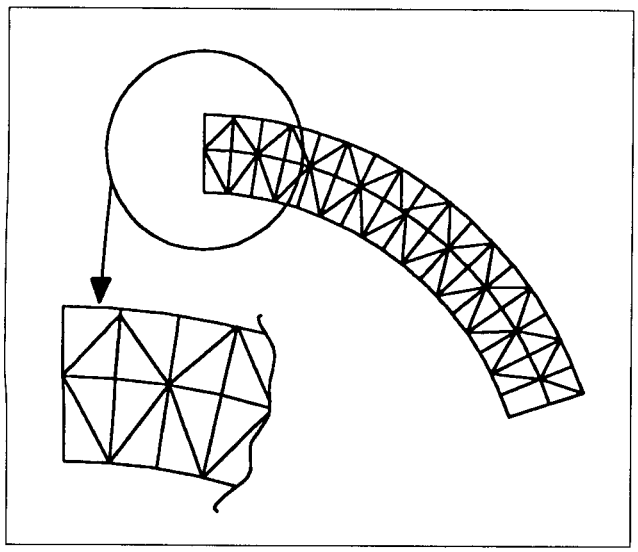

Figure 5. The finite element model of part of the monolayer cylinder.

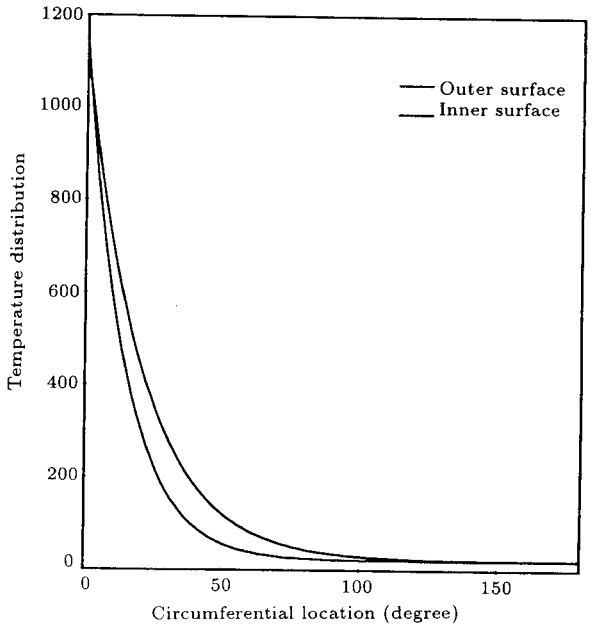

Figure 6. Radial temperature distribution due to cooling of weld in inner and outer surface.

The value of the resistance for a tightly wrapped vessel was taken from Armstrong and Jawad [13] to be 850 W/m^2°K. Boundary conditions for the thermal stress analysis are shown in Figure 4.

NUMERICAL RESULTS

Heat Transfer Results

Figure 6 shows the distribution of the temperature around the circumference of the layer in the outer and inner surface, respectively. The maximum temperature occurs in the welding region. The temperature would sharply decrease as one distances from the welding zone. As shown in these figures, the difference in temperature on the inner and outer layer is considerable up to an angle of around 45°. For angles more than 45°, the difference is slowing down smoothly up to nearly no difference for angles more than 120°.

Figure 7 shows the temperature distribution in the wall thickness for different angles as one distances from the welding zone. As this figure shows, one can see that the difference in the temperature of the inner and outer layers would increase in the neighborhood of the welding region. Whereas in the welding zone and in the regions far away from the welding zone, the inner and outer layers have almost identical temperature distribution.

Thermal Stress Results

Figure 8 shows the radial distribution of the tangential prestress due to cooling of the weld, averaged over the circumference of the model. Since the thickness of

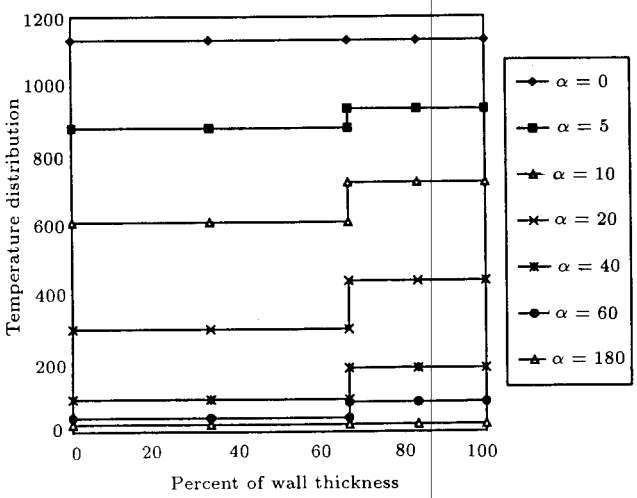

Figure 7. Radial temperature distribution due to cooling of weld.

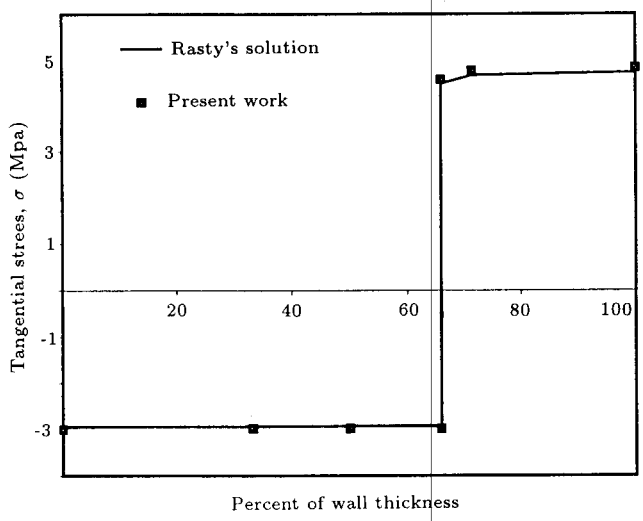

Figure 8. Radial distribution of the tangential prestress due to cooling of weld.

the core was twice that of the layer, 0%-67% of wall thickness shows the stress in the core, and 67%-100% of wall thickness shows the stress in the welded layer. As shown in this figure, the tangential prestress in the core is purely compressive, balanced by tensile prestress in the welded layer. For this case, the comparison is made with those of Rasty's method yielding a satisfactory agreement.

Figure 9 shows the circumferential distribution of the tangential stress at the outer and inner surfaces.

An analytical solution for determination of the magnitude of prestress throughout the wall thickness of a monolayer wrapped vessel has been reported [2]. In this calculation, it is assumed that the tangential and radial displacements are uniformly distributed around the circumferences of the layers. Figure 10 shows the distribution of the tangential displacement around the circumference of each layer. The tangential

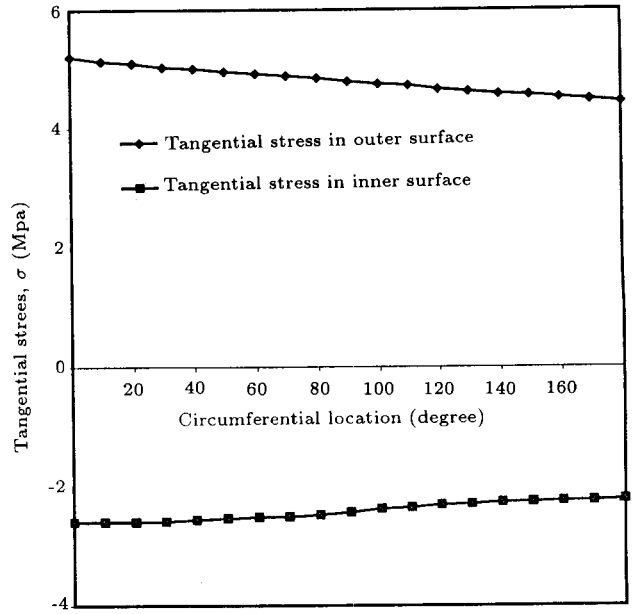

Figure 9. Circumferential distribution of the tangential prestress.

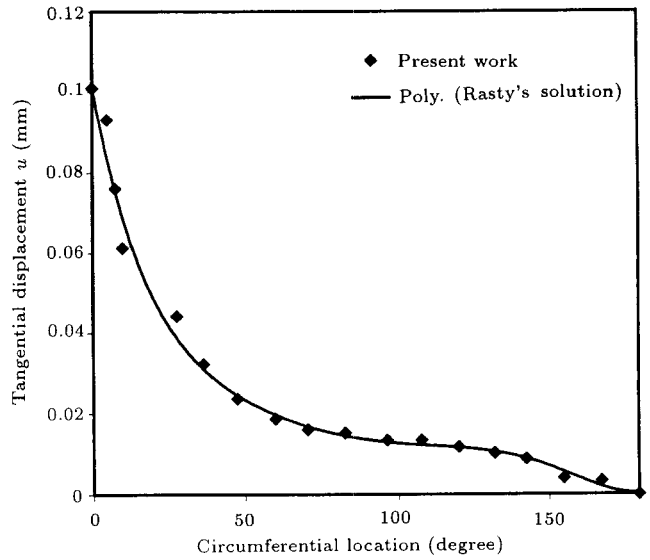

Figure 10. Circumferential distribution of the tangential displacement of the outer surface.

displacement obtained from the analytical solution is also plotted for comparison with the finite element results. It is interesting to note that the maximum value of the tangential displacement obtained from the finite element method is the same as that obtained from the analytical solution, however, at other points, the displacements would deviate from the analytical solution.

Figure 11 will show a comparison between the radial distribution of the tangential stress along the wall thickness resulted from the present work and the analytical solution. As this figure shows, the tangential

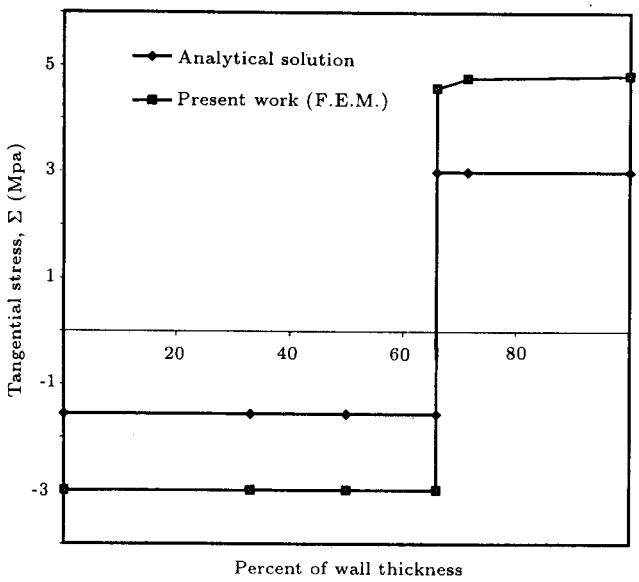

Figure 11. A comparison between radial distribution of the tangential stresses from the present work and those from analytical solution.

stress is of a compressive nature at the core and of a tensile nature at the layers. This figure shows that the magnitude of the tangential stress distribution, obtained from the finite element method, is consistently 50 percent larger than the magnitude of the stresses obtained from analytical solutions. This higher magnitude of stresses is mainly attributed to the simplification of the problem in analytical solution, which assumes that the tangential and radial displacements are uniformly distributed around the circumference of the layer.

CONCLUSION

In this paper, a formulation for the application of the finite element method for two-dimensional thermoelastic contact analysis of monolayer pressure vessels was presented. At the interfaces of the layers interface elements were employed. The interface elements developed were based on the formulation presented by Yuan and Chua [10], which were originally employed to study soil and structure foundation interaction.

REFERENCES

1. Srinivasan, M.G. and France, D.M. "Non-uniqueness in steady-state heat transfer in prestressed duplex tubes-analysis and case history", *ASME, J. Appl. Mech.*, **52**, pp 257-262 (1985).
2. Rasty, J. and Sabbaghian, M. "Effect of imperfect contact between adjacent layers on the integrity of wrapped vessels", *ASME, J. of Pressure Vessel Tech.*, **110**, pp 247-254 (1988).
3. Wang, Y., Soler, A.L. and Chen, G.L. "The self-rescue capacity of wrapped vessels- A theoretical and experimental analysis", *ASME, J. of Pressure Vessel Tech.*, **112**, pp 410-416 (1990).
4. Jahanian, S. and Sabbaghian, M. "Thermoelastoplastic and residual stresses in a hollow cylinder with temperature-dependent properties", *ASME, J. of Pressure Vessel Tech.*, **112**, pp 85-91 (1990).
5. Rasty, J. and Tamhane, P. "Application of the finite element method to quasi-static thermoelastic analysis of prestress in multilayer pressure vessels", *ASME, J. of Pressure Vessel Tech.*, **116**, pp 254-260 (1994).
6. Zibdeh, H.S. and Al Farran, J.M. "Stress analysis in composite hollow cylinder due to an asymmetric temperature distribution", *ASME, J. of Pressure Vessel Tech.*, **117**, pp 59-65 (1995).
7. Boley, B.A. and Weiner, J.H., *Theory of Thermal Stresses*, John Wiley and Sons Inc, New York (1960).
8. Goodman, R.E., Taylor, R.L. and Brekke, T.L. "A model for the mechanics of jointed rock", *ASCE J. Soil Mech. and Found. Div.*, **94**, pp 637-659 (1968).
9. Ghaboussi, J., Wilson, E.L. and Witherspoon, P.A. "Finite element for rock joints and interfaces", *ASCE J. Soil Mech. and Found. Div.*, **99**, pp 833-848 (1973).
10. Yuan, Z. and Chua, K.M. "Exact formulation of axisymmetric interface element stiffness matrix", *ASCE J. Soil Mech. and Found. Div.*, **118**, pp 1264-1271 (1992).
11. Barber, J.R. "Non-uniqueness and stability for heat conduction through a duplex heat exchanger tube", *J. Thermal Stresses*, **9**, pp 69-78 (1986).
12. Barber, J.R. "The influence of interface thermal contact resistance on the heat transfer performance of prestressed duplex tube", *Int. J. Heat Mass Transfer.*, **29**, pp 761-767 (1986).
13. Armstrong, W.P. and Jawad, M.H. "Evaluation of thermal conductivity in layered vessels", *ASME, J. of Pressure Vessel Tech.*, **103**, pp 307-313 (1981).

Scientia Iranica, Vol. 10, No. 1, pp 110–115

SCIENTIA
IRANICA

Research Note

Solution of Torsion Problem by Boundary Integral Equation and Wavelet Analysis

M. Nikkhah Bahrami*, M.H. Naei[1] and S. Momeni[1]

A new numerical method has been proposed by combining the boundary integral and spectral methods. In this method, similar to the boundary element method, shape functions are used to solve the integral equation. However, for the functions, an orthogonal basis called wavelet functions, is used. Combining these two methods, together with the use of wavelet functions, leads to a modified method. Through this method, the Poisson equation is solved for the torsion of prismatic bars and the distribution of the normal derivative of stress function is extracted.

INTRODUCTION

In this article, a new numerical method is proposed, which is a combination of the boundary element method and the spectral method. In the spectral method, a set of orthogonal functions, known as wavelet functions, are used for transferring the unknown quantities of the problem into a non-physical domain, e.g. the frequency domain. The two methods are presently regarded as independent methods and have great merits. It seems, however, that integrating the features of both methods is more useful than common numerical methods. The greatest merit of this method is seen in its use of wavelet functions, particularly in obviating the singularity of the fundamental solution. This problem has been the focus of a number of researchers who have tried to obviate the singularity of the fundamental solution used in the boundary integral method through analytical methods. In this method, however, this problem has been solved without the need for these mathematical techniques, by using wavelet functions. Taking into account the fact that there is no need for mashing of the solved area, the following are among the merits of this method:

- Definite convergence of the solution,
- Spectral accuracy of the solution,
- Continuity of the solution.

*. *Corresponding Author, Department of Mechanical Engineering, Tehran University, Tehran, I.R. Iran.*
1. *Department of Mechanical Engineering, Tehran University, I.R. Iran.*

In the next sections, the integral form of the Poisson equation is presented and then, wavelet functions and multi-resolution analysis is introduced. The last section presents the integration of the methods with the result of the solution.

INTEGRAL FORM OF POISSON EQUATION

This section introduces and discusses the integral form of the Poisson equation in the two-dimensional state.

The problem considered here is solving the following differential equation:

$$\nabla^2 u = h, \tag{1}$$

on the $\Omega \in R^2$ domain and with the boundary Γ, in such a way that h is harmonic, which means $\nabla^2 h = 0$ with a constant Dirichlet boundary condition. Γ is allowed to have a cusp, but the solution domain is singly connected. In general, the integral form of Equation 1 is as follows:

$$C(x)u(x) + \int_\Gamma \left[u(y)\frac{\partial w}{\partial n}(x,y) - w(x,y)\frac{\partial u}{\partial n} \right] d\Gamma(y) = \int_\Omega w(x,y)h(z)dv(z), \tag{2}$$

where $x(x_p, y_p) \in \Omega$, or $\Gamma, y(x_a, y_a) \in \Gamma, z(x_i, y_i) \in \Omega, w$ is the Green function and is obtained through the fundamental solution of the following equation:

$$\nabla^2 w + \delta(x,z) = 0 \quad x, z \in \Omega^\infty, \tag{3}$$